Mobile methane measurements: Effects of instrument specifications on data interpretation, reproducibility, and isotopic precision

Takriti, Mounir[a], Wynn, Peter M.[a], Elias, Dafydd[b], Ward, Susan E.[a], Oakley, Simon[b] McNamara, Niall P.[b]

[a]Lancaster Environment Centre, Lancaster University, Bailrigg, Lancaster, LA1 4YQ, UK

[b]UK Centre for Ecology and Hydrology, Lancaster Environment Centre, Library Avenue, Bailrigg, Lancaster, LA1 4AP, UK

Keywords: fugitive emissions; cavity ring-down spectroscopy; natural gas; greenhouse gases

Abstract

Recent research has used mobile methane (CH_4) measurements to identify and quantify emissions, but the effect of instrument response time on concentration measurements is rarely considered. Furthermore, stable isotope ratios are increasingly used in mobile measurements to attribute sources, but the precision of mobile isotopic measurements depend on a combination of instrument and measurement conditions. Here we tested the effect of instrument speed on concentration measurements by outfitting a vehicle with isotopic and concentration-only gas analysers with different response times and conducting multiple mobile surveys. Additionally, we performed a sensitivity analysis for the isotopic precision achievable under different conditions by programming a physical model, validated with empirical data from our mobile surveys. We found that slower response time led to a greater underestimation of measured CH_4 concentration, during both driving and stationary measurements, while the area under peaks in concentration is consistent and provides a robust means of comparing data between instruments. We also explore the use of an algorithm to improve instrument response. Our sensitivity analysis showed that the precision of isotopic measurements increases with the concentration range and the duration of the measurement following a power law. Our findings have important implications for the reporting and comparability of results between surveys with different instrumental setups and provide a framework for optimising sampling strategies under given objectives, conditions, and instrument capabilities.

1. Introduction

Atmospheric concentrations of methane (CH_4) have increased by more than 160 % since pre-industrial times and continue to rise. As CH_4 has 32 times the global warming potential of CO_2 (Etminan et al., 2016), there has been increasing focus on reducing emissions from anthropogenic sources, such as natural gas infrastructure, agriculture, and waste treatment. However, efforts to reduce emissions are still hampered by uncertainty around the location and contribution of different fugitive emission sources, and there is often considerable

disagreement between inventory estimates and atmospheric measurements (e.g. Turner et al., 2016).

Vehicle mounted mobile measurement systems, which use gas analysers based on infrared absorption spectroscopy, were used as early as the 1990s to quantify landfill CH_4 emissions (Czepiel et al., 1996). More recent advances in spectroscopic gas analysers have led to the increasing use of mobile systems to map CH_4 concentrations, detect fugitive emission sources, and quantify emission rates (e.g. Fischer et al., 2017; Jackson et al., 2014). The origin of emissions can be ambiguous, particularly if there are multiple emission sources in an area. Using analysers that measure CH_4 concentrations and $^{13}CH_4$ isotope ratios can help distinguish between emission sources. In particular, it becomes possible to distinguish between microbial sources, such as landfills or agricultural emissions, which are typically depleted in $^{13}CH_4$, and thermogenic sources, such as natural gas extraction and distribution, which are typically enriched in $^{13}CH_4$.

While mobile CH_4 measurements do not provide continuous data over time and roadway measured concentrations can strongly depend on meteorological conditions, they offer several advantages compared to point measurements or lab analysis of field samples: 1) High spatial resolution as CH_4 concentration can be mapped at a scale of meters; 2) good spatial coverage as, depending on road access, tens to hundreds of kilometres can be covered within days; 3) immediate detection of elevated concentrations enabling rapid investigation, e.g. response to gas leaks. This approach therefore offers wide applications within academic research, industry monitoring and maintenance, as well as regulatory oversight and compliance monitoring.

Instrument manufacturers have been developing systems that integrate sampling, gas analysis, navigation, and data processing, marketed primarily as turn-key solutions for leak detection in the natural gas industry. Both pre-built systems and user-built set-ups have been used for a variety of applications: tracer release studies to quantify emissions from waste water treatment plants (Yoshida et al., 2014) and landfills (Mønster et al., 2014); measuring fence line CH_4 and H_2S at gas wells (Eapi et al., 2014); attributing oil and gas emissions using $^{13}CH_4$ and C_2H_6 measurements; mapping urban gas pipeline leaks (Jackson et al., 2014) and estimating leak rates (Fischer et al., 2017); and assessing emissions from geological fault lines

(Boothroyd et al., 2016). The use of mobile survey systems may therefore increase in the future as spectroscopic gas analysers become more widely available, and new applications, such as operation on unmanned aerial vehicles, are explored (Allen et al., 2019). However, the published literature on mobile CH_4 measurements has mainly focussed on the dissemination of results, and while instrument setup and performance have been described in detail elsewhere (e.g. Rella et al., 2015a), the effects of instrument specifications on results obtained and their interpretation have rarely been discussed.

The range of instrumental setups used in mobile monitoring systems is increasing, and applications are moving from one-off surveying campaigns to routine monitoring of regional fugitive emissions (Albertson et al., 2016). It is thus essential to consider how hardware specifications will affect performance and suitability for different applications, particularly with regards to reproducibility and comparability of data.

Current mobile spectroscopic gas analysers, such as used in this study, measure concentrations with precisions in the ppb range. While this level of precision is generally sufficient for the requirements of mobile surveys, measured concentrations are not necessarily equal to atmospheric concentrations, due to a lag in instrument response.

The response time of an instrument consists of two components: the transit time and the rise time. Transit time is the time required for a volume of air to move from the air inlet to the analyser cavity. This can easily be corrected for when matching concentration and location data, and does not affect the measured concentration as such, although diffusive mixing of air in the sampling system will increase with increasing tube volume and decreasing flow rate.

The rise time is the time delay between an initial step change in gas concentration and the response in measured concentration of the analyser. It reflects the change in gas composition in the analyser cavity as the gas is replaced continuously while the instrument goes through measurement cycles, and is typically given as T_{90}, the time it takes for the measured concentration to reach 90% of the final concentration. When a step change in concentration occurs, the final concentration is only measured if it is sampled for the duration of the rise (or corresponding fall) time (Brunner and Westenskow, 1988). This can lead to underestimation of atmospheric concentrations in mobile measurements and impede comparability of results

obtained with different instrumental setups. The effect of rise time on gas concentration measurements has been previously explored for respiration measurements in clinical settings (Brunner and Westenskow, 1988; Schena et al., 1984; Tang et al., 2005) where mathematical corrections have been developed to improve instrument response (Arieli and Van Liew, 1981; Farmery and Hahn, 2000).

Additional considerations apply when using isotopic gas analysers to distinguish between emission sources: current mobile spectroscopic gas analysers measure $^{13}CH_4/^{12}CH_4$ ratios with two orders of magnitude lower precision than isotope ratio mass spectrometry (IRMS) systems (Zazzeri et al., 2015). Moreover, instrument precision is generally specified for averages of continuous measurements of a sample over a period of time, while mobile measurements are variable and typically use regression analysis, such as with Keeling or Miller-Tans plots, to derive source isotope signature estimates (e.g. Lopez et al., 2017; Rella et al., 2015a). The effective precision during mobile measurements thus depends on a variety of factors, including both instrument and emission characteristics.

Here, to investigate the effects of instrument response time on different measures of CH_4 emissions and their comparability between instruments, we compare concentration data produced by two different instruments using a custom-built mobile system built around an isotopic ($^{13}C/^{12}C$) CH_4 gas analyser, and a concentration-only CH_4 gas analyser. Additionally, we perform a sensitivity analysis using Monte Carlo simulations of a simple physical model to quantify the effects of instrument parameters and sampling conditions on the isotopic precision of mobile measurements. The model results were validated by comparing our empirical estimates of source signature precision with outputs of model simulations.

2. Materials and methods

2.1. Methane measurements

To evaluate the effect of instrument response time on CH_4 measurements in the field, a vehicle (Mitsubishi L200) was equipped with two gas analysers, a Picarro G2201-*i* isotopic gas analyser (Picarro Inc. Santa Clara, USA) and a Los Gatos Research Ultraportable Greenhouse Gas Analyzer (Los Gatos Research Inc., San Jose, USA), henceforth referred to as G2201-*i* and UGGA, respectively.

The G2201-*i* and the UGGA have a measurement frequency of 0.26 Hz and 1.2 Hz, and flow rates of 25 mL min^{-1} and 650 mL min^{-1}, respectively. The rise time, i.e. the time to reach 90% of the final concentration measurement in response to a step change in concentration (T_{90}) is 38 s for the G2201-*i* and 14 s for the UGGA. Both instruments measure CO_2, CH_4, and H_2O concentrations in air. The instrument specifications differ largely because they are optimized for different tasks and capabilities: the G2201-*i*'s lower flow rate enables more precise isotope measurements, whereas the UGGA is designed for applications that require a rapid response to concentration changes, such as flux measurements.

The air inlet was attached to the pole of the anemometer (see below) on the roof of the vehicle, with the opening facing downward and terminating in a cone to prevent water ingress. This air inlet was connected to the air inlet of the UGGA via a 310 cm nylon tube with an outer/inner diameter of 6 mm/3 mm. A PTFE air filter (Vacushield, Pall Life Sciences, MI, USA) was mounted on the inlet and airflow could be redirected via a solenoid valve to a drying column inside the vehicle during instrument shutdown or to protect the instrument from moisture intake. The two gas analysers were connected in series with the G2201-*i* air inlet connected to the UGGA air outlet (Figure 1). Excess air flow was vented via an open split. The output of each analyser was broadcast via Wi-Fi to two tablet devices mounted in front of the passenger seat so that measurements could be monitored in real time. The G2201-*i* was powered by five 72 Ah deep cycle batteries connected in parallel to a pure sine wave power inverter, other components used DC power from a single battery (Figure 1). All components were mounted on a wooden frame, with compartments for instruments and batteries, that was secured on the bed of the vehicle. The batteries provided enough charge to operate the system for over 10 h of continuous measurements. For electrical safety, fuses were installed between the batteries and the power inverter, as well as in the DC circuit. The AC system was grounded to the chassis of the vehicle.

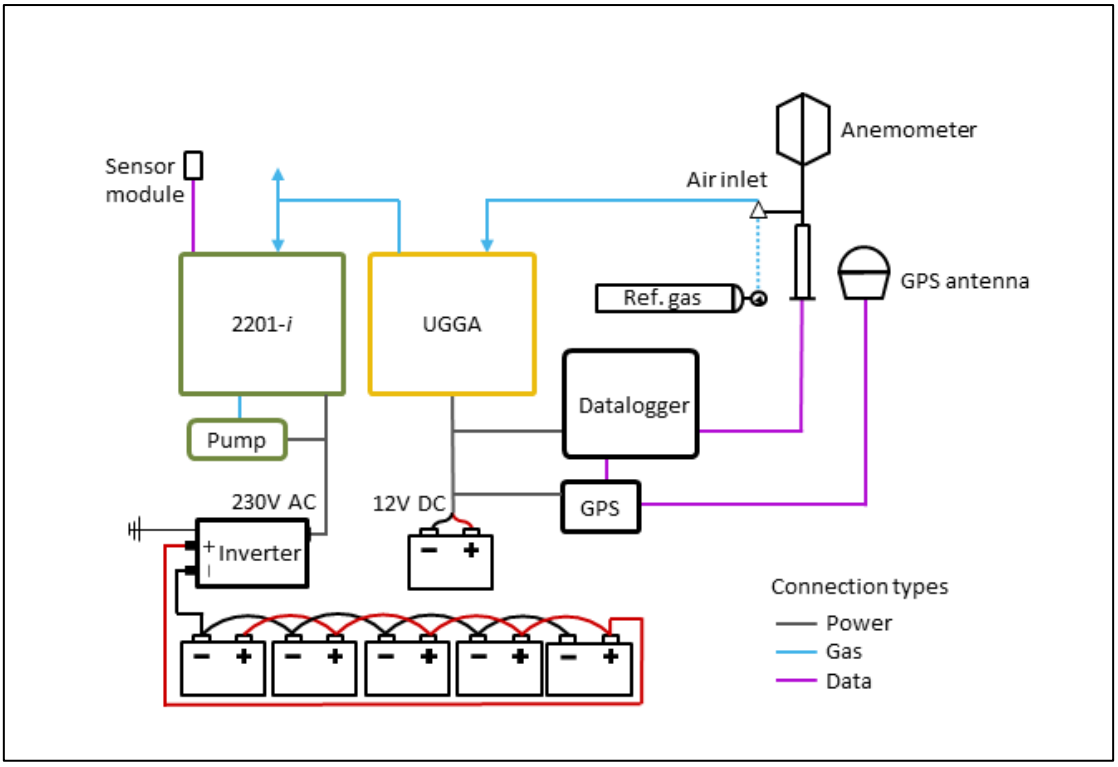

Figure 1 Schematic of mobile system built around a Picarro 2201-*i* isotopic gas analyser and a Los Gatos Research UGGA gas analyser. GPS is a Hemisphere R330 differential GPS, anemometer is a WindMaster PRO 3-Axis Ultrasonic Anemometer, sensor module contains an accelerometer and environmental sensors. Dotted line shows a temporary connection between the reference gas cylinder and the air inlet only used during drift checks.

2.2. Location and wind data

Location and speed were measured by a R330 GNSS Receiver with a Hemisphere A21 Antenna (Hemisphere GNSS Inc., Arizona, USA) mounted on the vehicle roof providing location data with a nominal accuracy of ≤ 0.5 m. Wind speed and direction were measured using a roof mounted WindMaster PRO 3-Axis Ultrasonic Anemometer (Gill Instruments Ltd. Hampshire, UK). Data from both instruments were recorded to a CR6 datalogger (Campbell Scientific, Loughborough, UK) at 10 Hz and calculations were made in post processing, see SI.

2.3. Laboratory testing

The transit time between the air inlet and the gas analysers was measured by connecting two reference gases to the air inlet via a three-way valve and measuring the delay in the change in concentration when switching from one reference gas to another. Gas passing through an instrument's cavity may be mixed and therefore affect subsequent measurements at the

outlet. To test if setting up the two gas analysers in series would affect measurements made by the G2201-*i*, standards with 3.03 ppm CH_4 and 10.1 ppm CH_4 were run through either just the G2201-*i* or both instruments, connected in series for 10, 30, 60, and 120 seconds. No significant differences in peak height, peak width, and peak area were found (paired t-test, n = 3, p-values > 0.3).

2.4. Standard calibration and drift check

Before surveys, the gas analysers were calibrated for concentration using certified standards with concentration of 3.03 ppm CH_4 and 10.4 ppm CH_4 (BOC Ltd., Guildford, UK) introduced through the system's air inlet. The G2201-*i* was calibrated for $\delta^{13}CH_4$ using isotopic standards with -23.9 ‰, -54.5 ‰, and -66.5 ‰ (Isometric Instruments, Victoria, Canada), covering the range of expected isotope ratios in the study area. Calibration standards were measured for 10 minutes each. To check for instrument drift during mobile surveys, a reference gas cylinder was mounted in the vehicle and gas was run through the sampling system immediately before, during, and after sampling campaigns for 10 minutes each. For individual sampling days, the standard deviations for mean CH_4 concentration measurements were 4 ppb for the UGGA and 0.9 ppb for the G2201-*i*, on average. Mean precision of $\delta^{13}CH_4$ measurements for individual sampling days was 0.73 ‰. Across all four sampling days, standard deviations were 14 ppb and 13 ppb, respectively, and precision was 0.74 ‰.

2.5. Field data collection

Field data were collected between November 2016 and March 2017 in the Fylde and Morecambe Bay areas in Lancashire and Cumbria, North West England, UK (54°00'N., 2°48'W, Figure 1). The area includes farmland, landfills, coastal wetlands, and natural gas processing and distribution infrastructure, and therefore a range of both biogenic and thermogenic emission sources. A total of 557 km was driven at a mean speed of 42 km h^{-1}. When encountering notably elevated CH_4 concentrations, the vehicle was stopped downwind for ~ 10 minutes, traffic conditions permitting, to improve precision of isotopic measurements.

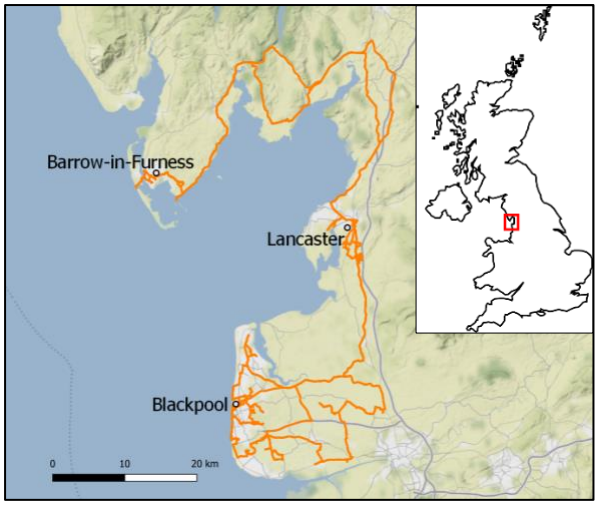

Figure 2 Overview of study area and route of surveys. Map insert shows location of study area within the UK.

2.6. Data analysis

2.6.1. Methane concentration analysis

For mobile surveys, what measurements count as an elevated concentration, or peak, has to be defined. The simplest approach is to use a fixed threshold and to define measurements above the threshold as peaks. However, background concentrations can vary between different areas and measurement times. Moving averages can therefore be more suitable unless a very conservative threshold is used. For example, Fischer et al. (2017) used a 2-minute rolling mean as a local background, and defined concentrations of either 10 % or 1 standard deviation ppm above that as elevated or peaks. Since our survey approach involved slowing down or stopping the vehicle for several minutes when encountering elevated concentrations, these prolonged measurements of higher concentrations would have influenced a rolling mean. We therefore instead chose to use a symmetric rolling 1st ventile (lowest 5%) over a 15-minute time window calculated separately for both gas analysers. This assumes that the lowest values at any given location will correspond to the background. To test the effect of threshold selection on results obtained we tested three different thresholds: 0.02 ppm (corresponding to 10 × and 52 × the standard deviations of instrument precision above the local background for the UGGA and G2201-*i* analysers, respectively), 0.1 ppm, and 0.3 ppm.

2.6.2. **Isotope analysis**

To determine the $\delta^{13}CH_4$ isotopic source signatures of emissions, a Miller-Tans plot was created for each peak. In this method, the isotope source signature is given as the slope of a regression of $\delta^{13}C \times [CH_4]$ and $[CH_4]$ (Miller and Tans, 2003). To determine the best fit line for the regression, we used York's method of regression for data with errors in both variables (York, 1969). This method was chosen over more conventional simple linear regression as it provides a more accurate unbiased estimate of the slope (Wehr and Saleska, 2017). The standard error (SE) of the slope was used to evaluate the precision of isotopic measurements. Given that the precision for a single measurement of the G2201-*i* is 3.01 ‰ (1 σ), numerous measurements at different concentrations are needed to obtain an accurate estimate of $\delta^{13}CH_4$ and so the source signature of smaller peaks cannot be accurately estimated. For this study, we therefore excluded all peaks with a standard error for the regression slope > 5 ‰. This threshold was chosen as it allows distinguishing between microbial sources of CH_4 (~ -62 ‰) and fossil sources of CH_4 ~ -43 ‰, Schwietzke et al., 2016) with confidence.

2.7. Isotope precision model and sensitivity analysis

2.7.1. **Model design**

To evaluate the effects of instrument specifications and plume characteristics on the precision of isotope measurements, we programmed a simple physical model to simulate gas measurements in the cavity of a spectroscopic gas analyser. As an exhaustive empirical analysis of the effects of these factors was not feasible, the model acts as a sensitivity analysis to better predict true precisions. The model generates a normally distributed gas peak with a given peak height (maximum concentration above background), isotope signature, and peak length (n_p), which represents the duration for which the peak is measured and therefore determines the number of measurements made (Figure 3). Assuming a measurement frequency of 1 Hz, a peak with $n_p = 60$ corresponds to passing a peak in 1 min. However, for the sake of general applicability, we defined parameters relative to dimensionless measurement cycles rather than units of volume or time. To account for the dilution of the peak with background air in the cavity, an exchange rate (*r*) is specified which gives the number of measurement cycles over which the gas in the cavity is completely replaced. For an instrument measuring at 1 Hz, this would correspond to the rise

time at which 100 % of the final concentration measurement is reached (T_{100}). This is modelled as a trailing moving average of length *r* and simulates the measurement of the air mixture in the cavity at any given time point. The total number of measurements per peak, n_t, is thus given as $n_t = n_p + r$. The gas peak is mixed with background air (1.91 ppm CH_4 at -47 ‰ $\delta^{13}C$) by calculating the true CH_4 concentration and $\delta^{13}C$ using a two-pool mixing model for each measurement point. Normal random noise is independently added to the CH_4 concentration and $\delta^{13}C$ with a mean of 0 and a standard deviation representing the instrument precision. Precision is assumed to be concentration independent. These are simplifying assumptions as random noise in concentration and $\delta^{13}C$ of spectroscopic measurements may be correlated (Wehr and Saleska, 2017) and concentration dependent (Rella et al., 2015a).

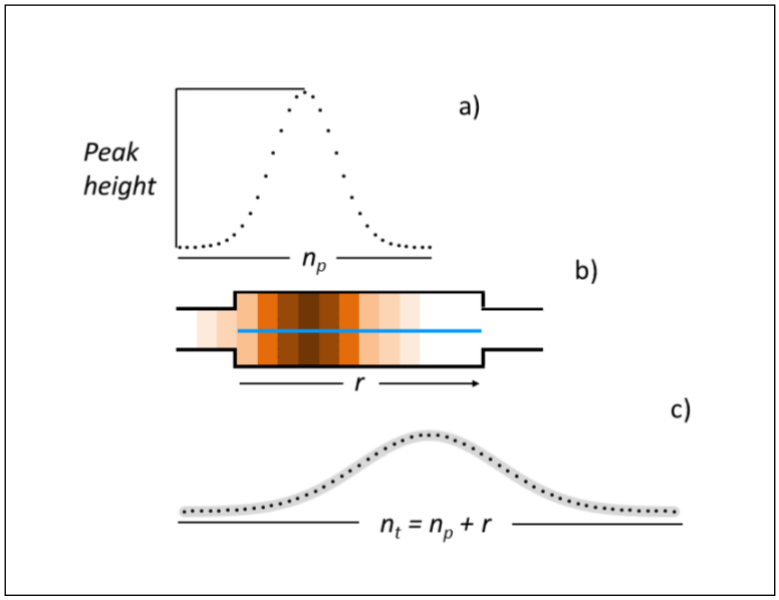

Figure 3 Graphical representation of isotope precision model, showing a) initial peak with true peak height (maximum concentration above background) and given peak length n_p relative to the number of measurement cycles (represented by points); b) representation of the instrument optical cavity and the gas concentration in it (horizontal blue line represents instrument laser and therefore the cavity length over which concentration is measured); and c) broadened peak as measured by the instrument with random noise added (grey overlay).

A York regression is applied to the set of measurements of each peak and the SE of the slope recorded as output. Monte Carlo simulations are run for sets of input parameters (see Table 2), performing 1,000 simulations for each combination of instrument precision, peak height, measurement duration (n_p), and instrument exchange rate (*r*).

The model, data processing, and analysis were coded in R version 3.4.3 (R Core Team, 2017), using the IsoplotR (Vermeesch, 2018) and MonteCarlo (Leschinski, 2017) packages. For isotope precision model code, see Takriti (2020).

2.7.2. **Model validation**

To validate the isotope precision model, we compared model output with SE estimates gathered from the mobile surveys with an SE < 10 ‰. The model was run with instrument precision set to that of our G2201-*i*, and peak height and n_p parameters set to those of observed peaks. The *r* parameter was set to 1 as the measured peaks had already been mixed in the cavity. There was very good agreement between simulated and empirical values with slope = 0.91, R^2 = 0.96 (**Error! Reference source not found.**). The model slightly underestimated SE, likely due to factors such as peak shape or other stochastic processes not considered by the model. For the empirical measurements, SE was proportional to $n^{-0.8}$ (**Error! Reference source not found.**).

3. Results and discussion

3.1. Instrument performance, concentration measurements, and data comparability

3.1.1. **Instrument response time**

When taking real time mobile measurements, where the sampled gas concentrations vary continuously, the rise time of the gas analysers used can affect the measured values. (Figure 4). The rise time depends on the cavity volume and the flow rate of the gas analyser. When an analyser is taking in a sample for less than the rise time (or correspondingly the fall time) the final concentration will not be reached. This is shown in Figure 4, where a 3.03 ppm CH_4 standard was run through the two instruments in series for either 10 s or 120 s, demonstrating how the instruments differ in transit time, rise time, and peak height. As air in the instrument cavity is continuously replaced, the measured concentration represents a mixture of incoming and present gas, such that the gas peak is broadened inversely proportional to the rate at which the gas is replaced. Hence, both instruments underestimate the true concentration at 10 s, but the faster analyser reaches a higher concentration in that timespan. However, the area under the curve of concentration over time is the same for both instruments.

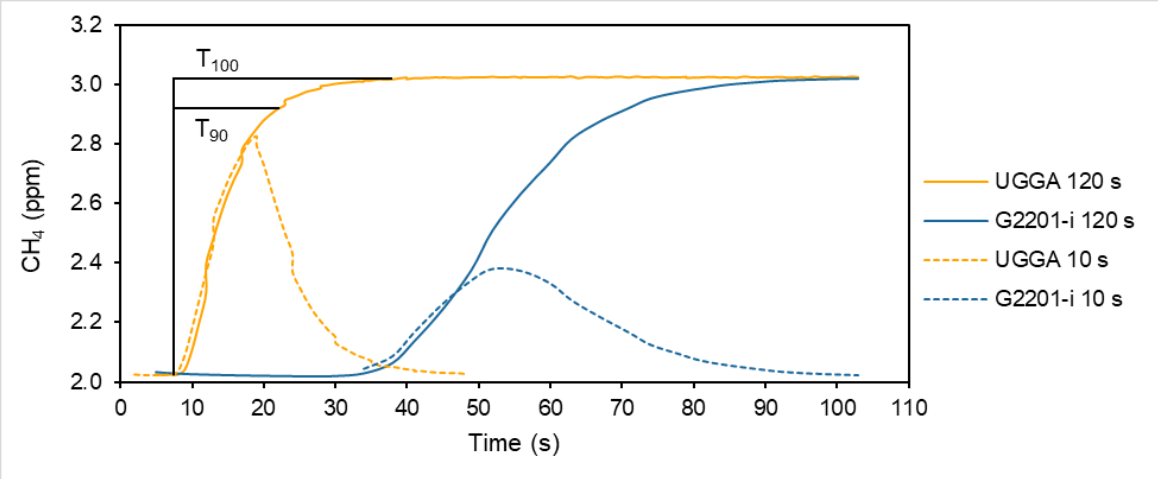

Figure 4 Concentration of a 3.03 ppm CH_4 standard gas as measured on a G2201-*i* isotopic gas analyser and a UGGA connected in series. Solid lines show measurements where the standard gas was connected for 120 s and both instruments reached stable readings. Dashed lines show measurements where the standard gas was connected for 10 s. Horizontal lines indicate rise times at which 90% (T_{90}) or 100% (T_{100}) of the final concentration have been reached for the UGGA.

3.1.2. **Methane concentrations**

To assess the effect of differing rise times under real world conditions, we compared CH_4 concentration measurements of the UGGA and G2201-*i* gas analysers from four sampling days. There was a consistent discrepancy in measured CH_4 concentration between the two gas analysers, with the G2201-*i* reporting lower concentrations (Figure 5). We plotted maximum peak concentrations measured by the two instruments against each other and found values from the G2201-*i* to be 40 % lower compared to the UGGA (Figure 6). This is a relative measurement, as the true peak concentrations are not known. The relationship between the peak concentrations of the two instruments was fairly stable throughout the surveys, and there was only a very weak positive relationship between the ratio of the G2201-*i* and UGGA peak heights and the driving speed (R^2 = 0.02, F(1, 224), p = 0.034). Therefore, differences in peak concentrations were still observed during stationary measurements, as demonstrated in **Error! Reference source not found.**, which shows concentration data collected over a ten-minute period in a parking lot close to a gas leak If sampled CH_4 concentrations are not constant, either due to micrometeorological variation or a moving sampling system, instruments may not report true concentrations unless their response was instantaneous. Such dependence of concentration measurements on rise time may lead to

underestimating emissions during mobile surveys, and limits the comparability of results, particularly when comparing data between instruments with significantly different rise times.

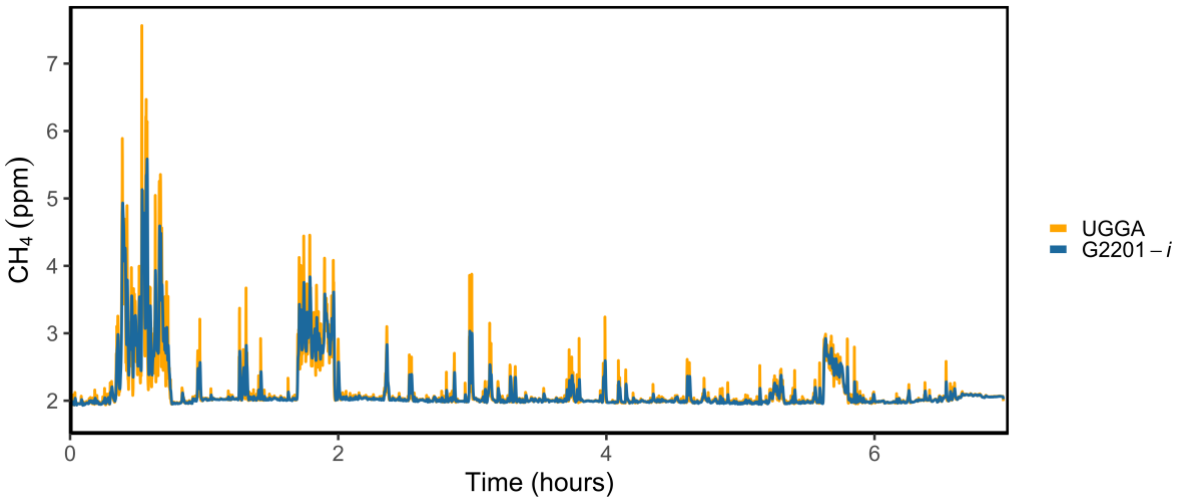

Figure 5 Mobile CH_4 measurements made simultaneously by a G2201-*i* isotopic gas analyser and a UGGA greenhouse gas analyser connected in series during mobile surveys. Only data points above background concentration for at least one of the analysers are shown.

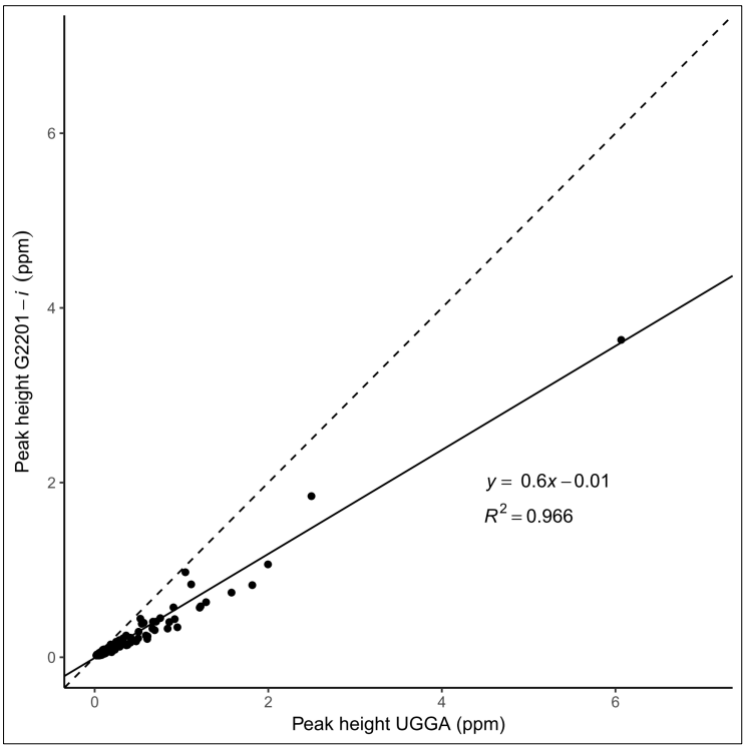

Figure 6 Maximum peak concentration above background for CH_4 peaks measured either by a G2201-i or a UGGA (n = 228). Peaks recorded by both analysers were matched if they overlapped temporally. In case of multiple overlapping peaks, the highest peak was selected. Dashed line shows slope = 1.

3.1.3. **Rise time correction**

To explore the potential for mathematical correction of rise times we adapted a correction algorithm based on a second order differential equation from Wong et al. (1998), developed by Arieli and Van Liew (1981), and applied it to standard gas measurements on our two instruments (see SI). For a step change in concentration, the algorithm reduced the effective rise time (T_{90}) by 42 % to 22 s for the G2201-*i* and 29 % to 10 s for the UGGA and reduced the associated underestimation in CH_4 concentrations (**Error! Reference source not found.**, **Error! Reference source not found.**). While amplifying noise in the measurements along with the signal, such methods may provide concentration values that are closer to true peak plume concentrations for mobile measurements.

3.1.4. **Peak count**

Another way to characterise emissions sources is to count the number of peaks, i.e. concentrations that exceed some threshold, encountered during mobile surveys of specific regions (Boothroyd et al., 2016). However, this measure is also dependent on instrument

response time, as any given threshold will be reached more quickly and therefore more frequently on a faster instrument. **Table 1** shows the number of CH_4 peaks above background levels for both instruments at three different thresholds. Depending on the selected threshold, around 60 % fewer peaks were detected on the G2201-*i* compared to the UGGA, due to the difference in response time. Selecting a higher threshold will mainly remove small and locally constrained emission plumes from the analysis but higher thresholds also eliminated peaks whose isotopic signature could be determined with sufficient precision, thus potentially eliminating useful data.

Table 1 Number of CH_4 peaks counted during mobile surveys at different thresholds with two gas analysers and the number of peaks whose $\delta^{13}CH_4$ signature could be estimated with a precision (SE) of < 5 ‰.

Threshold (ppm)	G2201-*i*	UGGA	G2201-*i*/UGGA	SE < 5 ‰
0.02	236	726	0.33	6
0.1	67	157	0.43	4
0.3	32	80	0.40	3

3.1.5. **Peak area**

While peaks measured by a slower instrument are broadened relative to those measured by a faster instrument, the peak area remains the same (Figure 4). When comparing peak areas obtained from mobile surveys, the UGGA would occasionally measure several distinct peaks for every one peak of the G2201-*i*. We accounted for this by adding temporally overlapping peak areas together. This resulted in a perfect relationship between the instruments, indicating that peak areas provide a robust means of comparing data between instruments (Figure 7). Peak areas will be sensitive to driving speeds as the measurement duration and therefore area increases with decreasing speed. However, since driving speed is known and peak area decreases linearly with speed, this can be corrected for (**Error! Reference source not found.**). Also, depending on the research question, peak areas may provide additional insight. For example, Fischer et al. (2017) found that peak areas are correlated with emission rate for urban gas pipeline leaks. Such relationships may exist for other sources and peak areas may thus aide quantification of emission rates.

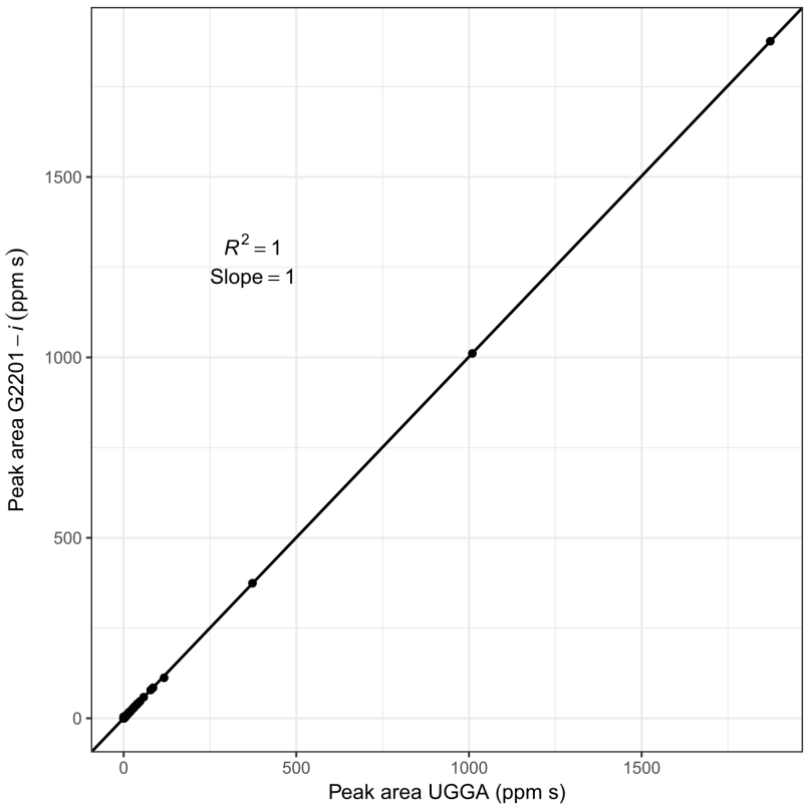

Figure 7 Scatter plot of peak CH_4 areas (n = 230) measured across four mobile surveys as measured by a G2201-i isotopic gas analyser and a UGGA greenhouse gas analyser connected in series.

3.2. Isotope precision model and sensitivity analysis

For mobile isotopic measurements, the isotopic signature is determined through regression analysis. The effective precision of the measurements therefore depends not only on the precision of the instrument and measurement duration, but also on factors such as the range of concentrations measured and the instrument response time. As exploring the relative importance of these effects experimentally is technically challenging, we programmed a physical model simulating gas flow through a spectroscopic analyser and used a Monte Carlo simulation to generate stochastic noise in the measurements, simulating random error.

We ran the model with all possible combinations of parameters, namely instrument precision, peak height above background, measurement duration (n_p), and instrument exchange rate (r). For isotopic precision, we used settings approximating the performance of our G2201-*i*, as well as settings of hypothetical instruments with higher precision. For the CH_4 plume parameters, we used a range of values representative of data collected during our surveys or those reported in the literature.

As would be expected, the precision of plume measurements increases linearly with the isotopic precision of the analyser (Table 2). Both isotopic and concentration measurement precision influence the precision estimate of plume isotope measurements. However, since the precision of concentration measurements of current spectroscopic CH_4 analysers is around four orders of magnitude higher than the precision of isotopic measurements, improving concentration precision has negligible effects (data not shown), and was therefore kept constant for all model iterations.

Peak height, i.e. the maximum concentration of the plume above background, also had a strong effect on isotopic precision as it extends the range of both variables in the Miller-Tans regression model. Because isotopic precision of gas analysers may increase with concentration, our model may slightly underestimate the improvement in precision. Increasing n_p (i.e. increasing measurement duration) also decreases SE, such that SE is minimised by increasing both peak height and n_p. The relationship between SE and peak height and SE and n_p are both described by power functions (**Error! Reference source not found.** & **Error! Reference source not found.**), meaning that for the practical domains, initial improvements in either of these parameters will lead to large improvements in isotopic precision. However, approaching the asymptote any further will only result in marginal precision improvements. For practical applications, it may therefore not be possible to fully compensate for low plume concentrations by increasing the measurement time, e.g. by taking stationary downwind measurements. Increasing r, i.e. the rise time of the instrument, increases n_t, and therefore the number of measurements per peak, but it also increases response time and effectively reduces the measured maximum concentration. As outlined above, this may have a significant effect on SE depending on the values of n_p and the initial peak height. Such trade-offs occur e.g. when using AirCore technology where sampled gas is captured in a narrow tube during mobile surveys, and then "replayed" at a slower speed to increase the precision of the isotopic measurements (Karion et al., 2010; Rella et al., 2015b).

Overall, our model demonstrates that for a given set of instrument parameters, achieved isotopic precision will heavily depend on both plume concentration and measurement duration. For example, increasing concentration from 1 ppm CH_4 to 2.5 ppm CH_4 above background while increasing n_p from 100 to 250 (corresponding to an increase from ~6.5 min to ~16 min at 0.26 Hz) reduces uncertainty more than threefold (Table 2).

Table 2 Results of Monte Carlo simulations of the effects of instrument and plume parameters on the precision of simulated $\delta^{13}CH_4$ plume measurements. Parameters: precision is instrument precision given as 1σ for a single isotopic measurement, *r* is number of measurement cycles over which gas in the instrument cavity is replaced, n_p is measurement cycles, peak height is max peak concentration above background. Simulations of plume measurements for each parameter combination were repeated 1000 times. Precision of $\delta^{13}CH_4$ measurements is calculated as mean standard error for the slope of a Miller-Tans plot using York regression.

			Peak height (ppm)							
Precision (‰)	*r*	n_p	0.5	1	2.5	5	7.5	10	15	20
3.0	20	100	3.81	2.13	1.13	0.78	0.66	0.60	0.53	0.50
		250	2.35	1.33	0.71	0.50	0.42	0.39	0.35	0.32
		500	1.66	0.94	0.50	0.35	0.30	0.27	0.25	0.23
		1000	1.18	0.67	0.36	0.25	0.21	0.19	0.17	0.16
	40	100	4.26	2.33	1.17	0.78	0.65	0.58	0.51	0.47
		250	2.37	1.33	0.71	0.49	0.42	0.38	0.34	0.32
		500	1.66	0.94	0.50	0.35	0.30	0.27	0.24	0.23
		1000	1.18	0.66	0.36	0.25	0.21	0.19	0.17	0.16
	60	100	4.91	2.62	1.25	0.80	0.64	0.56	0.49	0.44
		250	2.44	1.36	0.71	0.49	0.42	0.38	0.33	0.31
		500	1.66	0.94	0.50	0.35	0.30	0.27	0.24	0.23
		1000	1.17	0.66	0.35	0.25	0.21	0.19	0.17	0.16
1.5	20	100	1.90	1.06	0.56	0.39	0.33	0.30	0.27	0.25
		250	1.17	0.66	0.35	0.25	0.21	0.19	0.17	0.16
		500	0.83	0.47	0.25	0.18	0.15	0.14	0.12	0.11
		1000	0.59	0.33	0.18	0.13	0.11	0.10	0.09	0.08
	40	100	2.12	1.16	0.58	0.39	0.32	0.29	0.25	0.23
		250	1.18	0.67	0.35	0.25	0.21	0.19	0.17	0.16
		500	0.83	0.47	0.25	0.18	0.15	0.14	0.12	0.11
		1000	0.59	0.33	0.18	0.12	0.11	0.10	0.09	0.08
	60	100	2.45	1.31	0.63	0.40	0.32	0.28	0.24	0.22
		250	1.22	0.68	0.36	0.25	0.21	0.19	0.17	0.16
		500	0.83	0.47	0.25	0.17	0.15	0.14	0.12	0.11
		1000	0.58	0.33	0.18	0.12	0.11	0.10	0.09	0.08
0.5	20	100	0.63	0.35	0.19	0.13	0.11	0.10	0.09	0.08
		250	0.39	0.22	0.12	0.08	0.07	0.06	0.06	0.05
		500	0.27	0.15	0.08	0.06	0.05	0.05	0.04	0.04
		1000	0.19	0.11	0.06	0.04	0.04	0.03	0.03	0.03
	40	100	0.70	0.38	0.19	0.13	0.11	0.10	0.08	0.08
		250	0.39	0.22	0.12	0.08	0.07	0.06	0.06	0.05
		500	0.27	0.15	0.08	0.06	0.05	0.05	0.04	0.04
		1000	0.19	0.11	0.06	0.04	0.04	0.03	0.03	0.03
	60	100	0.81	0.43	0.21	0.13	0.11	0.09	0.08	0.07
		250	0.40	0.22	0.12	0.08	0.07	0.06	0.06	0.05
		500	0.27	0.15	0.08	0.06	0.05	0.04	0.04	0.04
		1000	0.19	0.11	0.06	0.04	0.04	0.03	0.03	0.03

4. Conclusions

It is important to consider how instrument setup and sampling conditions can affect the results of mobile measurements. We show that slower instrument response time can lead to a significant underestimation of mobile concentration measurements. This should be taken into account when comparing absolute values across different setups, and we therefore recommend consistently reporting instrument rise time for mobile applications. While mathematical corrections may improve concentration estimates, our results demonstrate that peak areas of emission plumes are independent of instrument response times and provide an alternative and more robust means to compare data obtained between different instrument setups. Additionally, we show that isotopic precision of mobile measurements determined with regression methods is not just a function of instrument precision, but also instrument speed, measurement duration and, importantly, concentration range. The model we developed can predict these effects on isotopic precision for any given instrumental setup and application. It can therefore inform choices on equipment used, as well as sampling strategies, and estimate expected uncertainty. As the underlying principles are independent of chemical species, our findings are relevant to applications other than CH_4 measurements, such as mobile air pollution measurements (Apte et al., 2017) or the emerging field of unmanned aerial vehicle based measurement systems.

5. Acknowledgements

M.T. was funded by a Lancaster University Faculty of Science and Technology PhD studentship. N.P.M. was funded by the Natural Environment Research Council award number NE/R016429/1 as part of the UK-SCAPE programme delivering National Capability. We acknowledge the UK-SCAPE Flux tower network. We thank Natalie Davis for her input and help in preparation of this manuscript, we further thank Deirdre Kerdraon-Byrne and James Edgerley for assistance with data collection.

6. References

Albertson, J.D., Harvey, T., Foderaro, G., Zhu, P., Zhou, X., Ferrari, S., Amin, M.S., Modrak, M., Brantley, H., Thoma, E.D., 2016. A Mobile Sensing Approach for Regional Surveillance of Fugitive Methane Emissions in Oil and Gas Production. Environ. Sci. Technol. 50, 2487−2497. https://doi.org/10.1021/acs.est.5b05059

Allen, G., Hollingsworth, P., Kabbabe, K., Pitt, J.R., Mead, M.I., Illingworth, S., Roberts, G., Bourn, M., Shallcross, D.E., Percival, C.J., 2019. The development and trial of an unmanned aerial system for the measurement of methane flux from landfill and greenhouse gas emission hotspots. Waste Manag. 87, 883–892. https://doi.org/10.1016/j.wasman.2017.12.024

Apte, J.S., Messier, K.P., Gani, S., Brauer, M., Kirchstetter, T.W., Lunden, M.M., Marshall, J.D., Portier, C.J., Vermeulen, R.C.H., Hamburg, S.P., 2017. High-Resolution Air Pollution Mapping with Google Street View Cars: Exploiting Big Data. Environ. Sci. Technol. 51, 6999–7008. https://doi.org/10.1021/acs.est.7b00891

Arieli, R., Van Liew, H.D., 1981. Corrections for the response time and delay of mass spectrometers. J. Appl. Physiol. 51, 1417–1422.

Boothroyd, I.M., Almond, S., Worrall, F., Davies, R.J., 2016. Assessing the fugitive emission of CH4 via migration along fault zones – Comparing potential shale gas basins to non-shale basins in the UK. Sci. Total Environ. https://doi.org/10.1016/j.scitotenv.2016.09.052

Brunner, J.X., Westenskow, D.R., 1988. How the rise time of carbon dioxide analysers influences the accuracy of carbon dioxide measurements. Br. J. Anaesth. 61, 628–638. https://doi.org/10.1093/bja/61.5.628

Czepiel, P.M., Mosher, B., Harriss, R.C., Shorter, J.H., McManus, J.B., Kolb, C.E., Allwine, E., Lamb, B.K., 1996. Landfill methane emissions measured by enclosure and atmospheric tracer methods. J. Geophys. Res. 101, 16711. https://doi.org/10.1029/96JD00864

Eapi, G.R., Sabnis, M.S., Sattler, M.L., 2014. Mobile measurement of methane and hydrogen sulfide at natural gas production site fence lines in the Texas Barnett Shale. J. Air Waste Manage. Assoc. 64, 927–944. https://doi.org/10.1080/10962247.2014.907098

Etminan, M., Myhre, G., Highwood, E.J., Shine, K.P., 2016. Radiative forcing of carbon dioxide, methane, and nitrous oxide: A significant revision of the methane radiative forcing. Geophys. Res. Lett. 43, 12,614-12,623. https://doi.org/10.1002/2016GL071930

Farmery, A.D., Hahn, C.E., 2000. Response-time enhancement of a clinical gas analyzer facilitates measurement of breath-by-breath gas exchange. J. Appl. Physiol. 89, 581–589.

Fischer, J.C. von, Cooley, D., Chamberlain, S., Gaylord, A., Griebenow, C.J., Hamburg, S.P., Salo, J., Schumacher, R., Theobald, D., Ham, J., 2017. Rapid, Vehicle-Based Identification of Location and Magnitude of Urban Natural Gas Pipeline Leaks. Environ. Sci. Technol. 51, 4091–4099. https://doi.org/10.1021/acs.est.6b06095

Jackson, R.B., Down, A., Phillips, N.G., Ackley, R.C., Cook, C.W., Plata, D.L., Zhao, K., Philips, N.G., Ackley, R.C., Cook, C.W., Plata, D.L., Zhao, K., 2014. Natural gas pipeline leaks across Washington, DC. Environ. Sci. Technol. 48, 2051–8. https://doi.org/10.1021/es404474x

Karion, A., Sweeney, C., Tans, P., Newberger, T., 2010. AirCore: An Innovative Atmospheric Sampling System. J. Atmos. Ocean. Technol. 27, 1839–1853. https://doi.org/10.1175/2010JTECHA1448.1

Leschinski, C.H., 2017. MonteCarlo: Automatic Parallelized Monte Carlo Simulations.

Liu, S., Yang, X., Zhou, X., 2020. Development of a low-cost UAV-based system for CH 4 monitoring over oil fields. Environ. Technol. 0, 1–10. https://doi.org/10.1080/09593330.2020.1724199

Lopez, M., Sherwood, O.A., Dlugokencky, E.J., Kessler, R., Giroux, L., Worthy, D.E.J., 2017. Isotopic signatures of anthropogenic CH4 sources in Alberta, Canada. Atmos. Environ. 164, 280–288. https://doi.org/10.1016/j.atmosenv.2017.06.021

Miller, J.B., Tans, P.P., 2003. Calculating isotopic fractionation from atmospheric measurements at various scales. Tellus, Ser. B Chem. Phys. Meteorol. 55, 207–214. https://doi.org/10.1034/j.1600-0889.2003.00020.x

Mønster, J.G., Samuelsson, J., Kjeldsen, P., Rella, C.W., Scheutz, C., 2014. Quantifying methane emission from fugitive sources by combining tracer release and downwind measurements - a sensitivity analysis based on multiple field surveys. Waste Manag. 34, 1416–28. https://doi.org/10.1016/j.wasman.2014.03.025

R Core Team, 2017. R: A Language and Environment for Statistical Computing.

Rella, C.W., Hoffnagle, J., He, Y., Tajima, S., 2015a. Local- and regional-scale measurements of CH_4, $\delta^{13}CH_4$, and C_2H_6 in the Uintah Basin using a mobile stable isotope analyzer. Atmos. Meas. Tech. 8, 4539–4559. https://doi.org/10.5194/amt-8-4539-2015

Rella, C.W., Hoffnagle, J., He, Y., Tajima, S., 2015b. Local- and regional-scale measurements of CH4, Δ13CH4, and C2H6 in the Uintah Basin using a mobile stable isotope analyzer. Atmos. Meas. Tech. 8, 4539–4559. https://doi.org/10.5194/amt-8-4539-2015

Schena, J., Thompson, J., Crone, R.K., 1984. Mechanical influences on the capnogram. Crit. Care Med. 12, 672–674. https://doi.org/10.1097/00003246-198408000-00015

Schwietzke, S., Sherwood, O.A., Bruhwiler, L.M.P., Miller, J.B., Etiope, G., Dlugokencky, E.J., Michel, S.E., Arling, V.A., Vaughn, B.H., White, J.W.C., Tans, P.P., 2016. Upward revision of global fossil fuel methane emissions based on isotope database. Nature 538, 88–91. https://doi.org/10.1038/nature19797

Takriti, M., 2020. Isotope precision model. https://doi.org/10.5281/zenodo.3748490

Tang, Y., Turner, M.J., Baker, A.B., 2005. Effects of lung time constant, gas analyser delay and rise time on measurements of respiratory dead-space. Physiol. Meas. 26, 1103–1114.

https://doi.org/10.1088/0967-3334/26/6/019

Turner, A.J., Jacob, D.J., Benmergui, J., Wofsy, S.C., Maasakkers, J.D., Butz, A., Hasekamp, O., Biraud, S.C., 2016. A large increase in U.S. methane emissions over the past decade inferred from satellite data and surface observations. Geophys. Res. Lett. 43, 2218–2224. https://doi.org/10.1002/2016GL067987

Vermeesch, P., 2018. IsoplotR: A free and open toolbox for geochronology. Geosci. Front. https://doi.org/10.1016/j.gsf.2018.04.001

Wehr, R., Saleska, S.R., 2017. The long-solved problem of the best-fit straight line: application to isotopic mixing lines. Biogeosciences 14, 17–29. https://doi.org/10.5194/bg-14-17-2017

Williams, E., 2011. Aviation Formulary v1.46 [WWW Document]. URL http://www.edwilliams.org/avform.htm (accessed 5.11.18).

Wong, L., Hamilton, R., Palayiwa, E., Hahn, C., 1998. A real time algorithm to improve the response time of a clinical multigas analyser. Algorythm 14, 441–446. https://doi.org/10.1023/A:1009941900141

York, D., 1969. Least squares fitting of a straight line with correlated errors. Earth Planet. Sci. Lett. 5, 320–324. https://doi.org/10.1016/S0012-821X(68)80059-7

Yoshida, H., Mønster, J.G., Scheutz, C., 2014. Plant-integrated measurement of greenhouse gas emissions from a municipal wastewater treatment plant. Water Res. 61, 108–18. https://doi.org/10.1016/j.watres.2014.05.014

Zazzeri, G., Lowry, D., Fisher, R.E., France, J.L., Lanoisellé, M., Nisbet, E.G., 2015. Plume mapping and isotopic characterisation of anthropogenic methane sources. Atmos. Environ. 110, 151–162. https://doi.org/10.1016/j.atmosenv.2015.03.029